

Quasi-Steady Aerodynamic Model for Bat Airframes

Model Version 1.1, dated 30 January 2012

R. D. Bullen¹ and N. L. McKenzie²

¹ 43 Murray Drive Hillarys Western Australia 6025, Australia – bullen2@bigpond.com

² Department of Environment and Conservation, PO Box 51, Wanneroo, Western Australia 6946, Australia

INTRODUCTION

Estimates of bat flight energetics begin with the calculation of the mechanical power required by the airframe to maintain steady (unaccelerated) level flight. Previous models (e.g. Norberg *et al.* 1993 for bats and Pennycuik 2008 for birds) do not provide realistic power-velocity polars for the array of airframe types represented in Western Australian bat communities.

Here we derive a quasi-steady aerodynamic model for bats, including justification of various airframe-specific coefficient values applicable to each term in the power, wing inertia and lift/drag equations, where these are not already published. We recognise that this model may only be appropriate in the range of flight speeds between 'stall' and maximum, where airflow patterns can be approximated using quasi-steady assumptions.

No "linear" model coefficient values are available for the unsteady aerodynamics that bats are known to use at their lowest flight speeds (Muijres *et al.* 2008). Furthermore, compared to solving the complex, computationally expensive Navier-Stokes equations that describe unsteady flow patterns (Persson *et al.* 2011), especially those around the variable geometries associated with a bat's airframe during its wing-beat cycle, quasi-steady models are straight forward to apply and may be sufficient for many analyses.

This webpage presents our calculations of the four components of the mechanical power element of the 'velocity/power curve' (induced, profile, parasitic and inertial power). We make this model available for further testing and refinement by scientists/students working on bat aerodynamics and foraging energetics who have their own empirical flight speed, metabolic and airframe data.

THE MECHANICAL POWER MODEL

We expand the methods of Pennycuik (1969), Weis-Foch (1972), Tucker (1973), Norberg *et al.* (1993), Rayner (1999) and Grodzinski *et al.* (2009) to calculate the mechanical power required by various bats across a range of 7-Feb-12flight speeds. This power is supplied directly by the flight muscles (primarily the pectoral girdle and the upper arm muscles) to allow the bat to maintain steady (unaccelerated) level flight. The method applies the 'quasi-steady' aerodynamic assumptions applicable for the speed range between 'stall' and 'maximum level', but not down to 'hover'. The model calculates the contributions to the power curve in steady, level, forward flight of: induced (or lift-dependent) drag, profile wing drag, the parasitic drag of the ears, head, body, feet, tail and inner wing (when

immersed in the wake of the ears), and wingbeat inertia. The equation for calculating flight mechanical power at any given flight speed (Norberg *et al.* 1993) is:

$$P_{\text{mech}} = P_{\text{ind}} + P_{\text{pro}} + P_{\text{par}} + P_{\text{int}} \quad \dots\dots\dots (1)$$

Its four elements are calculated using data on:

- airframe morphology (including geometry, wing inertia),
- aerodynamic cleanliness attributes (including lift and drag coefficients), and
- dynamic factors (such as wingbeat frequency and amplitude at various speeds).

1. Induced Power Calculation

The ‘Induced Power’ component is required to overcome the induced (or lift dependent) drag at a given speed. From aerodynamic theory, the drag induced by the wing/body/head/tail is well understood and is given in Hoerner (1965) as:

$$C_{D \text{ ind}} = C_L^2 (1 + \delta) / (\pi AR) \quad \dots\dots\dots (2)$$

Where C_D , C_L and AR represent drag coefficient, lift coefficient and wing-body aspect ratio, respectively. Herein we adopt a value for δ of 0.2 after Pennycuick (1975, 1989) and Grodzinski *et al.* (2009). This is because bats have lifting bodies and near-elliptical wing-planforms (Bullen & McKenzie 2007), and the flight speeds where the induced drag contribution is most interesting are those just above the minimum flight speed of the wing. Induced power is:

$$P_{\text{ind}} = D_{\text{ind}} V \quad \dots\dots\dots (3)$$

where V is the flight speed of the bat, and after Norberg *et al.* (1993), Pennycuick (2008) and Grodzinski *et al.* (2009):

$$P_{\text{ind}} = [(m g / V_w)^2] (1 + \delta) V / (\rho S_{\text{wd}} 2) \quad \dots\dots\dots (4)$$

where S_{wd} is the wing disk area ($= \pi b_{\text{ref}}^2 / 4$) and V_w is the average resultant airspeed over the wing.

Following (Norberg *et al.* 1993), V_w can be estimated from strip theory by resolving the forward flight speed of the bat and the local wing speed perpendicular to the forward velocity vector ($v_{\text{strip}} = b_{\text{strip}} \theta_w f_w$). We take the resultant velocity of the wrist ($v_{\text{wr}} = b_{\text{wr}} \theta_w f_w$) to represent an average value that is used for the entire wing, so V_w is given from:

$$V_w^2 = (V^2 + v_{\text{wr}}^2) \quad \dots\dots\dots (5)$$

2. Wing Profile Power Calculation

Rayner (1999) argues that reliable estimates of wing profile drag are required for accurate profile power calculation, the power to overcome the profile drag of the flapping wing at any given speed. For this calculation we include the area of the tail membrane in the wing area, because these membranes act in combination during flight. Again applying the quasi-steady aerodynamic assumption, profile power can be calculated using:

$$P_{\text{pro}} = q * S_{\text{w+ht}} * C_{D \text{ pro}} * V_w \quad \dots\dots\dots (6)$$

This parameter is primarily dependent upon the local lift coefficient (C_{l_w}) along the wing, the amount of camber present and the Reynolds Number (Re) at which the wing is operating. For the principle of similarity of forces and moments to apply, test results for lifting models should be compared at a similar Re . Bats typically operate at Re between 5,000 and 100,000 (Bullen and McKenzie 2007). Schmitz (1942) gives data for the profile drag of a thin plate with 6% camber at $Re = 42,000$. The relevance of these data to bat aerodynamics is discussed in Bullen and McKenzie (2007). Unlike a number of previous studies that have used a constant value for wing profile drag for all lift coefficients below $C_{L_{max}}$, we used a drag relationship that varies as lift coefficient increases. For the majority of the bats studied, the cambered airfoil drag coefficient at C_{l_w} of 0.8 corresponds to a minimum value of 0.025. As speed increases towards maximum, roughly corresponding to $C_{l_w} \sim 0.05$, the lift coefficient drops toward zero and the drag coefficient increases toward 0.05, primarily due to adverse aerodynamic effects on the concave side of the airfoil generating unwanted trailing edge separation. Alternatively as speed drops toward 'stall' and C_{l_w} approaches $C_{L_{max}}$ the drag coefficient again raises, this time due to adverse effects on the trailing edge of the convex side. Our study does not attempt to model situations outside these two limits, i.e. where C_{l_w} is greater than $C_{L_{max}}$ or less than 0.0. Herein, the relationship is given in Figure 1.

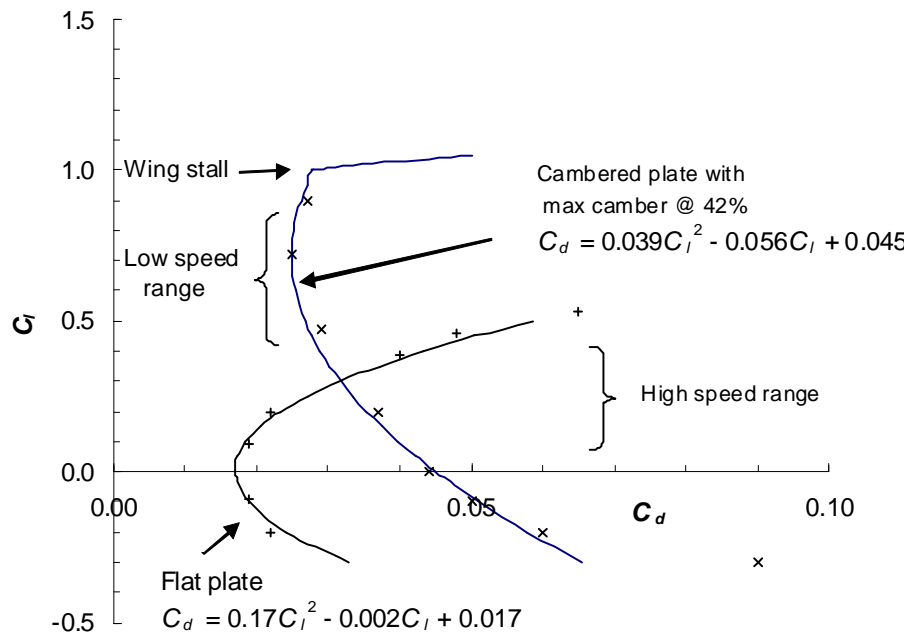


Figure 1. Two-dimensional airfoil drag polar for a cambered and a flat plate with sharp leading edges. Data is from Schmitz (1942) for $Re = 42,000$. The data points and the curve fit represent quasi-steady aerodynamic situations but not the unsteady, discontinuous wake, airflow conditions at very low flight speeds, between 'stall' and 'hover'.

We include the profile drag model for a flat airfoil in Figure 1, also from Schmitz (1942). The most obvious effects of reducing camber is to reduce the $C_{L\ max}$ at low speed, and to delay flow separation on the underside of the wing at high speeds and very low angles of attack.

It is important to allow for variation in lift and drag resulting from wing camber variation and control. While assessing the wing camber of live Western Australian (WA) *Mormopterus* spp we noted that they were able to completely straighten digit-5, including the intrinsic camber that is characteristic of the Metacarpal-5 in all other WA bat genera. For the *Mormopterus* calculations at high speed, where profile drag dominates, we used the flat airfoil model from Figure 1. In earlier publications we have noted that *Mormopterus*, unlike other Australian genera, has two distinct flight modes etc. While the other genera visibly modify the deployment of their tail, ear, wing camber and wing angle of attack to optimise their aerodynamics for different circumstances, as yet, none have shown the dual flight modes apparent in *Mormopterus* spp (Bullen and McKenzie 2002; McKenzie and Bullen 2009). Thus, from Figure 1,

$$\text{Cambered airfoil } C_d = 0.039 C_1^2 - 0.056 C_1 + 0.045 \quad @ Re = 42,000 \text{ with } C_1 \text{ between } 0 \text{ and } 1 \dots (7)$$

$$\text{Flat airfoil } C_d = 0.17 C_1^2 - 0.002 C_1 + 0.017 \quad @ Re = 42,000 \text{ with } C_1 \text{ between } 0 \text{ and } 0.5 \dots (8)$$

These two curves provide a more realistic model of high-speed wing profile drag than the constant value used by many previous authors. Wing profile drag dominates the power equation at these speeds and, without this lift-dependant relationship, the power could be underestimated by 30 to 60% resulting in unrealistically high maximum speed estimates.

$C_{d\ pro}$ is corrected for Re using the data from the thin, turbulent flow airfoil sections from Schmitz (1942) and Simmons (1999), as presented in Figure 2:

$$\Delta C_{d\ Re} = -0.0038 \text{Ln}(Re/1000) - \text{Ln}(42) \dots (9)$$

These three equations (from Figures 1 and 2) apply only for attached, steady flow, i.e. where $C_{1\ w}$ (the wings 3D lift coefficient) is greater than zero but less than its maximum value at ‘stall’ ($C_{1\ max}$).

$C_{1\ w}$ must be estimated before $C_{d\ pro}$ can be calculated.

$$C_{1\ w} = L_w / (q S_w) \dots (10)$$

Where L_w in steady level flight is the lift from the wing and tail remaining after the lift-contributions of the ears, head and body are subtracted from the weight of the bat:

$$L_w = (m_{bat} g) - (L_{ear} + L_{head} + L_{body}) \dots (11)$$

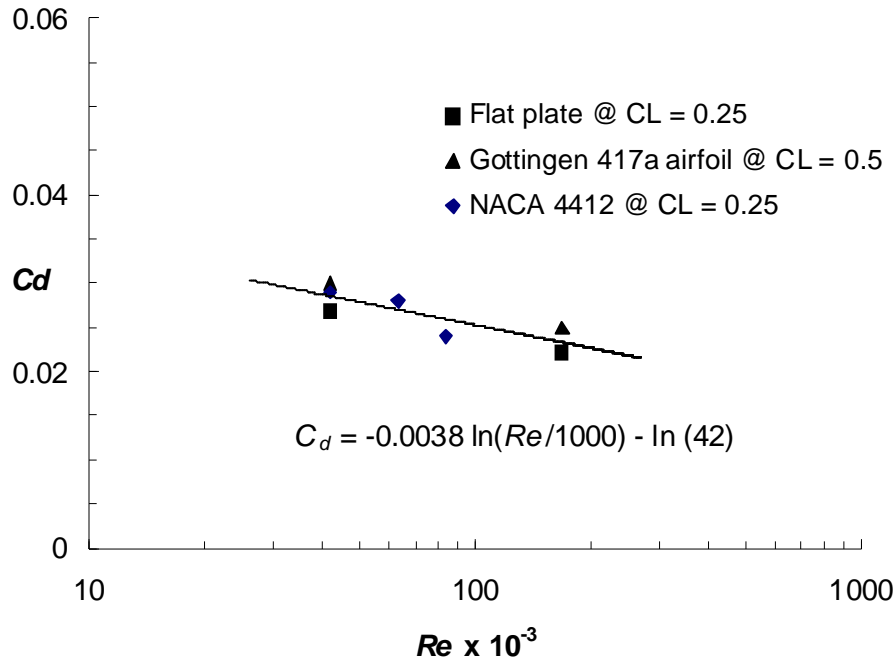


Figure 2. Variation of wing airfoil section drag coefficient with Re . Data are for thin airfoils with minimum camber and turbulent flow characteristics. Data are from Schmitz (1942) and Simmons (1999). The slope of the regression is $-0.0038 \ln(Re/1000)$.

L_{ear} , L_{head} and L_{body} are calculated using $C_l = 0.8$ at low speeds as all dorsal surfaces are cambered and can produce lift, except for 'ear type 0' (for ear type definitions and an explanation of the aerodynamic implications of different ear shapes, see Bullen and McKenzie 2009). Wind tunnel data presented in Gardiner *et al.* (2008) show that type-3 ears, if sufficiently rigid, may generate lift up to half the total weight of the bat at moderate flight speeds ($4 - 6 \text{ m s}^{-1}$), and potentially, its full weight at high speeds ($> 6 \text{ m s}^{-1}$). However, our observations on this type of bat show that they reduce the angle of attack of their ears at moderate and high flight speeds (Bullen and McKenzie 2009, p. 9). Also, the positive camber that characterise the dorsal surfaces (ears, head and body) of bat airframes (Bullen and McKenzie 2001, 2009), even those with short-ears, will generate sufficient lift to support a percentage of the bat's weight. Consequently, we limit this lift sub-total ($L_{\text{ear}} + L_{\text{head}} + L_{\text{body}}$) to a quarter of the bat's weight at moderate to high speeds.

3. Parasitic Power Calculation

Prior to modeling the parasitic power contributions of the bat's airframe, other than the wing, the aerodynamic cleanliness and size of the various lifting surfaces must be assessed. The parasitic power component to overcome the drag of the ears, head, and body is calculated by summing contributions from these surfaces (after Hoerner 1965):

$$P_{\text{para}} = q * V_{\text{true}} * \Sigma (C_{\text{D para-appendage}} * S_{\text{appendage}}) \dots\dots\dots (12)$$

3.1 Appendage Parasitic Drag Contributions

The drag coefficients of the various appendages were discussed in detail by Bullen and McKenzie (2009). In summary:

$C_{\text{D para-head/body}} = 0.4$, the general value based on the body maximum cross-sectional area; from Pennycuick *et al.* (1988) for air superiority and gleaning bats. This value is higher than the 0.08 recommended by Pennycuick (2008) for birds in flight, but is at the upper limit of values applied by various authors for bats (0.1, Grodzynski *et al.* 2009; 0.4, Norberg *et al.* 1993 & Pennycuick 2008, p. 51). The higher value is more applicable to bats that are not particularly aerodynamically clean, to account for their open mouths, nostrils, furry pelage and the lack of blending of their heads with their shoulders and backs.

= 0.25 for aerodynamically clean bats with silky fur (i.e. Western Australian molossids and emballonurids, Bullen and McKenzie 2008).

= 0.5 for surface bats with the woolly fur, because it interferes with ear wake ("long-eared" bats: *Nyctophilus*, *Macroderma*).

= 1.0 for species with bristly or velour-like fur. These have a much higher drag value because of the extreme aerodynamic roughness of their fur (*Hipposideros ater*).

$C_{\text{D para-ears}} = 0.04$, the general value, based on the planform area of both ears, for bats with ear types-0, -1 and -2 (i.e. the bats with interceptor and air superiority airframes). This figure was set conservatively low on the assumption that these short-eared bats will normally align their ears to the airflow in such a way as to provide the required lift while minimising the drag and maintaining hearing. The value was extrapolated from Schmitz (1942) curved-plate data at very low *Re* of 10,000.

= 1.0 for bats with ears that generate separated vortex flow (i.e. bats with type-3 ears, such as *Nyctophilus* and *Macroderma*). This is the value given in Hoerner (1965) for cylinders inclined to the airflow. It is reduced to 0.1 at higher flight speeds, where these bats align their ears with the local airflow.

= 2.0 for bats with type-4 ears (large ears without sculpted leading edges, such as *Hipposideros* spp). They are slow fliers so are not impaired by high parasitic drag, and do not attempt to generate the additional lift that would be needed to approach hover. Their ears are designed for optimal hearing characteristics.

$C_{\text{D para-tail}} = 0.05$, the general value based on the planform area of the tail membrane (S_{ht}). This figure is calculated as twice the skin-friction drag coefficient of the tail membrane, which should be similar to the skin-

friction of the wing membrane (~0.025, Schmitz 1942). The factor of two is assumed to take into account the 'tail lift'-dependant drag component.

= 0.2 for “long-eared” bats (with ear type-3) to account for surface interference from the bat’s back and tail membrane as the ear wake sweeps rearward.

$C_{D \text{ para-inner wing}} = 0.20$ for “long-eared” bats where the wakes from the outer edges of its type-3 ear’s sweep backward over the inner wing. This value is derived from Hoerner (1965, p. 6-13, figure 17) for wing sections with separated flow at low Re . It is based on the planform area of wing immersed in the wake of the ears. The inner wing area is taken as 10 % of the total wing area.

3.2 Appendage Area Calculations

Models from Bullen and McKenzie (2009) are used to calculate the $S_{\text{appendage}}$ contributions of body, tail and ears.

S_{body} The body cross-sectional area is given by the area of an ellipse, with width (w_{body}) and thickness (t_{body}) values derived from Bullen and McKenzie (2009, figure 2) as a function of head and body length ($l_{\text{head+body}}$):

$w_{\text{body}} = 51\%$ of $l_{\text{head+body}}$ for surface insectivores, 42% for interceptor and air superiority insectivores, and 30% for phytophagic bats such as *Pteropus*.

$t_{\text{body}} = 22\%$ for all bats.

Note that $l_{\text{head+body}}$ can be estimated from bat mass (m_{bat}) using the equation: $l_{\text{head+body}} = 0.285 m_{\text{bat}}^{0.346}$

$S_{\text{ear}} = K * \log_{10} m_{\text{bat}}$, where $K = 85$ for ear type-0 and -2 (all air superiority bats), 330 for type-1A (low aspect ratio interceptor ears of large molossids: *Tadarida*, *Chaerephon*), 180 for type-1B ears (high aspect ratio interceptor ears of small molossids such as *Mormopterus*), and 450 for type-3 and -4 (long-eared bats including *Hipposideros*, *Macroderma* and most *Nyctophilus* spp)

S_{ht} is the planform areas of the uropatagium for the bat groups. It is estimated for all tail types using the following equations (for tail type definitions and an explanation of the aerodynamic implications of different tail shapes, see Bullen and McKenzie 2009):

= $0.0180 * m_{\text{bat}}^{0.517}$ for air superiority and surface bats with tail types-1 and -3.

= $0.0146 * m_{\text{bat}}^{0.602}$ for interceptor bats with tail type-2. To allow for their documented ability to retract their tail membrane for high speed flight (Bullen and McKenzie 2009), this value is reduced by a further 70% at these speeds (i.e. = $0.0044 * m_{\text{bat}}^{0.602}$).

= $0.0094 * m_{\text{bat}}^{0.782}$ ($r^2 = 0.99$) for fruit and blossom bats with tail type-4.

4. Inertial Power Calculation

The ‘inertial power’ for each wingbeat is required to accelerate the mass of the pectoral girdle, arm and hand-wings during the first and third quarters of the wingbeat, and to decelerate them during the second and fourth quarters. A percentage of this power is then recovered as useful work, primarily by the generation of thrust during the down stroke, and by the recovery of potential energy into the bat’s muscles during the deceleration phases of the wingbeat (Norberg *et al.* 1993).

For this calculation, we applied a simplified wing-flapping model consistent with the quasi-steady aerodynamic model for forward flight:

The time of the wingbeat $T = 1 / f_w$ (sec / cycle) (13)

The total angle swept by the stroke = $2 \theta_w$ (14)

Average angular velocity about the shoulder/clavicle = $2 \theta_w f_w$ (15)

From data presented in Bullen and McKenzie (2002) for steady level flight conditions, the maximum angular velocity ($\omega_{max} = 2 \theta_w f_w \sqrt{2}$) occurs approximately at wings level ($\theta = 0$). Therefore, the maximum angular acceleration of the wing (approximately constant during the beat) is:

$$\begin{aligned} \omega_{tot\ max} &\sim \omega_{max} / (T / 4) \\ &\sim 8 \theta_w f_w^2 \sqrt{2} \\ &\sim 11.31 \theta_w f_w^2 \quad \dots\dots\dots (16) \end{aligned}$$

So the 'total inertial power' output (P_{int} in Watt) is the wing inertial torque (= angular acceleration * Inertia of the wing about its rotation origin) divided by time:

$$P_{int} = 11.31 I_w \theta_w f_w^3 \quad \dots\dots\dots (17)$$

But only 40% of the 'total inertial power' is converted to useful work in forward flight (Norberg *et al.* 1993, for *G. soricina*), therefore:

$$P_{int} \sim 6.78 I_w \theta_w f_w^3 \quad \dots\dots\dots (18)$$

WINGBEAT FREQUENCY AND AMPLITUDE MODEL

The wingbeat frequency (f_w) and amplitude (θ_w) values, required by equation (18), are calculated using the model presented in Bullen and McKenzie (2002):

$$f_w = 5.54 - 3.068 \log_{10} m_{bat} - 2.857 \log_{10} V \quad \dots\dots\dots (19)$$

$$\theta_w = 56.92 + 5.18V + 16.06 \log_{10} S_{ref} \text{ (degrees)} \quad \dots\dots\dots (20)$$

These relationships apply to all families of bats represented in Western Australia for the flight speed range between the usual minimum (V_{min} , analogous to stall speed) and the maximum flight speed. In the case of θ_w , the maximum values do not exceed the anatomical limit of 140° to 150° controlled by shoulder morphology (Bullen and McKenzie 2002).

WING INERTIA MODEL

The moment of inertia of each wing (I_w) is required by equation (18). The moment about the shoulder joint ($I_{w\ sh}$) is calculated following the 'strip' method described in Tholleson and Norberg (1991) for preserved specimens of each of the bats from the Coolgardie fauna (Bullen and McKenzie 2001) plus a group of tropical Western Australian bats. These inertia data were calculated using wing-strips delineated perpendicular to the quarter chord line of the stretched wing (the line that roughly approximates the axis of the bones forming the wing main spar: comprising the humerus, radius and digit-3). Figure 3 compares our results to the curve derived by Tholleson and Norberg (1991), whose data were derived using the stretching method of Norberg and Rayner (1987) that does not straighten the wing's main spar. Our curve is approximately 70% higher because corresponding wing-strips are

further from the bat’s shoulder. A representative curve for a single wing about the shoulder joint for modeling purposes is:

$$I_{w\ sh} = 0.0035 m_{bat}^{1.623} \dots\dots\dots (21)$$

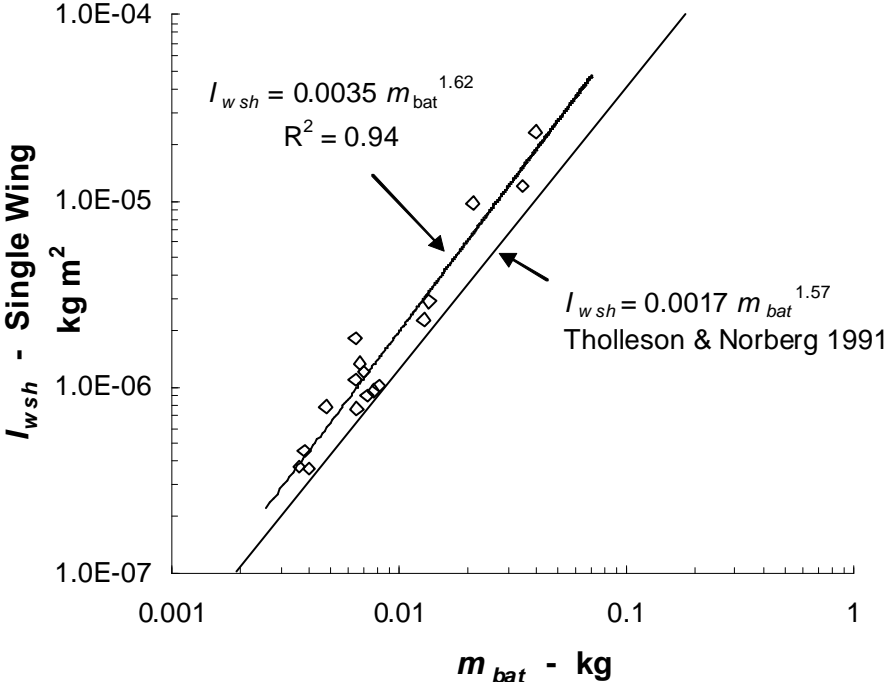


Figure 3. Moment of inertia of the wing about the shoulder joint: $I_{w-sh} = 0.0035 * m_{bat}^{1.62}$. Data from this study are compared with the curve from Tholleson and Norberg (1991). The *circa*.70% difference is due to the different method of stretching the wing reference line spanwise.

Altenbach and Hermanson (1987) found that bats have a scapulo-humeral lock in place during the top half of the downstroke, so the the wing rotates about the proximal end of the clavicle. Geometrically, the increase in inertia of the wing about the inboard end of the clavicle over the value about the shoulder is approximately 40%. Since the wing rotates about the shoulder joint during the bottom half of the downstroke, we assume that the average value of wing inertia to be applied to the calculation of P_{int} in equation (18) should be increased by 20%, therefore:

$$I_w = 1.2 * I_{w\ sh} \dots\dots\dots (22)$$

CALCULATION OF MAXIMUM LIFT ($C_{L\ max}$)

The lowest flight speed to which this quasi-steady model applies is analogous to the stall speed. This velocity value can be calculated from a bat’s morphology, and a $C_{L\ max}$ value appropriate to its airframe configuration derived. In the context of bat airframe morphologies, the factors that influence $C_{L\ max}$ were explored by Bullen and McKenzie (2007, 2009), and three classes were identified:

1. Experimental data in Schmitz (1942) yielded a $C_{L \max}$ of 1.05 for a thin cambered plate with a sharp leading-edge at a Re of 42,000. This combination of airfoil and low- Re corresponds to the bat airframes assigned to class 1 (short-eared bats with average leading-edge flap geometry) flying in steady level flight at high angle-of-attack with attached airflow.
2. Short-eared bats with broad leading-edge flaps. Emballonurids and pteropids assessed by Bullen and McKenzie (2007) have wide leading-edge flaps (12 to 18% of wing chord) that extend from the bat's shoulder to the base of its second phalanx, more than 80% of the wing's span. Data from Newsome *et al.* (1982) give an increase in $C_{L \max}$ for such flaps of between 0.1 and 0.5, depending on the spanwise extent of the flap. At the Re relevant to these bats, this equates an increment of about 0.25, giving a $C_{L \max}$ value of 1.3. We do not correct for the small increase in profile drag at the low speeds associated with $C_{L \max}$ because the drag calculation is dominated by induced drag at these speeds.
3. Long-eared bats with 3-dimensional vortex-generating ears. At low flight speed and high angles-of-attack, the lift possible from bats with type-3 ears depends greatly on the orientation of the ears and the creation of vortices from their leading edges. This is primarily controlled by the shape and sweep angle of the leading edge. Lift coefficients approaching 2.0 are possible for highly swept (70°) leading edges (Polhamus 1984). These values apply to the planform area of the delta wing, including the head, body and the section of the main wing that is swept by the vortices. In these flight conditions, the outer wing can also generate a 3-dimensional lift increment from high rates of change in angle of attack during the wing-beat cycle; even for rigid unflapped airfoils this property of dynamic stall, known as Kramer's effect, yields local lift coefficients at low- Re well in excess of 2.0 (e.g. Bousman 2000; Wolken-Mohlmann *et al.* 2007), because the airflow remains attached to the foil far longer than in a static condition. The inherent elasticity of bat wing bones and membranes (e.g. Swartz *et al.* 2007) offers the ability to take full advantage of this opportunity. The maximum lift coefficient used for these 'long-eared' bats is 2.0 (after Bullen and McKenzie 2009).

SYMBOLS AND SUBSCRIPTS

Symbols

AR	aspect ratio
b	span (m)
C_D	three dimensional lifting surface drag coefficient = $2 D / \rho / S_{ref} / V^2$
C_d	two dimensional airfoil section drag coefficient
C_L	three dimensional lifting surface lift coefficient = $2 L / \rho / S_{ref} / V^2$
C_l	two dimensional airfoil lift coefficient
D	drag (N)
f_w	wingbeat frequency (Hz)
g	acceleration due to gravity = 9.81 m s^{-2}
I	wing flapping inertia (kg m^2)
L	lift (N)
m	bat mass (kg)
P	Power (W)
q	dynamic pressure = $\frac{1}{2} \rho V^2$ (N m^{-2})
Re	Reynolds number
r^2	Pearson's correlation coefficient
S	area of a lifting or dragging surface or body (m^2)
T	time (s)
t	thickness, e.g. body thickness (m)
V	bat flight speed (m s^{-1})
v	local airflow velocity (m s^{-1})
w	width, e.g. body width
θ	wingbeat amplitude – empirical above or below the body axis reference dorsal plane (degrees)
ρ	air density = 1.2256 kg m^{-3} at sea level and 15° C
ω	wingbeat angular velocity (rad s^{-1})
$(1+\delta)$	induced drag factor accounting for effect of non-elliptical wing spanwise lift distribution

Subscripts

body	body
dot	acceleration
ear	ear
head	head
h/t	tail membrane (uropatagium)
ind	indicated
int	inertial
max	maximum condition
mech	mechanical
pro	profile
par	parasitic
ref	reference condition
sh	shoulder
true	true airspeed
w	wing
wd	wing disc (area)
wr	wrist

REFERENCES

- Altenbach, J.S. and Hermanson, J.W. (1987). Bat flight muscle function and the scapular-humeral lock. In: *Recent Advances in the Study of Bats* (eds Fenton M.B., Racey P.A. and Rayner J.M.V), pp 101–118. Cambridge University Press, Cambridge.
- Bousman, W.G. (2000). Airfoil dynamic stall and rotorcraft maneuverability. NASA TM-2000-209601.
- Bullen, R.D. and McKenzie, N.L. (2001). Bat airframe design: flight performance, stability and control in relation to foraging ecology. *Australian Journal of Zoology* **49**, 235–262.
- Bullen, R.D. and McKenzie, N.L. (2002). Scaling bat wingbeat frequency and amplitude. *Journal of Experimental Biology* **205**, 2615–2626.
- Bullen, R. D. and McKenzie, N. L. (2007). Bat wing airfoil and planform structures relating to aerodynamic characteristics. *Australian Journal of Zoology* **55**, 237–247.
- Bullen, R. D. and McKenzie, N. L. (2008). The pelage of bats (Chiroptera) and the presence of aerodynamic riblets: the effect on aerodynamic cleanliness. *Zoology (Jena, Germany)* **111**, 279–286.
- Bullen, R.D. and McKenzie, N.L. (2009). Aerodynamic cleanliness in bats. *Australian Journal of Zoology* **56**, 281–296.
- Gardiner, J., Dimitriadis, G., Sellers, W. and Codd, W. (2008). The aerodynamics of big ears in the brown long-eared bat *Plecotus auritus*. *Acta Chiropterologica* **10**, 313–322.
- Grodzinski, U., Spiegel, O., Korine, C. and Holdreid, M.W. (2009). Context dependant flight speed: evidence for energetically optimal flight speed in the bat *Pipistrellus kuhlii*. *Journal of Animal Ecology* **78**, 540–548.
- Hoerner, S.F. (1965). *Fluid Dynamic Drag*. Hoerner Fluid Dynamics, New Jersey.
- McKenzie, N.L. and Bullen, R.D. (2009). The echolocation calls, habitat relationships, foraging niches and communities of Pilbara microbats. *Records of the Western Australian Museum Supplement* **78**, 123–155.
- Muijres, F.T., Johansson, L.C., Barfield, R., Wolf, M., Spedding, G.R. and Hedenström, A. (2008). Leading-edge vortex improves lift in slow-flying bats. *Science* **319**, 1250–1253.
- Newsom, W. A., Satran, D. R. and Johnson, J. L. (1982). Effects of wing leading edge modifications on a full-scale, low-wing general aviation airplane. NASA Technical Paper 2011.
- Norberg, U. M. and Rayner, J. M. V. (1987). Ecological morphology and flight in bats (Mammalia: Chiroptera): Wing adaptations, flight performance, foraging strategy and echolocation. *Philosophical Transactions of the Zoological Society of London B* **316**, 335–427.
- Norberg, U.M., Kunz, T.H., Steffensen, J.F., Winter, Y. and Von Helversen, O. (1993). The cost of hovering and forward flight in a nectar-feeding bat, *Glossophaga soricina*, estimated from aerodynamic theory. *Journal of Experimental Biology* **182**, 152–153.
- Pennycuik, C.J. (1969). The mechanics of bird migration. *Ibis* **111**, 525–556.
- Pennycuik, C.J. (1975). Mechanics of flight. In: *Avian Biology* (eds Farner, D.S. and King, J.R.). Academic Press, New York.
- Pennycuik, C.J. (1989). *Bird Flight Performance: A Practical Calculation Manual*. Oxford University Press, Oxford.
- Pennycuik, C.J. (2008). *Modelling the Flying Bird*. Academic Press, London, UK.

- Pennycook, C.J. Obrecht, H.H. and Fuller, M.R. (1988). Empirical estimates of body drag of large waterfowl and raptors. *Journal of Experimental Biology* **135**, 253–264.
- Persson, P.-O., Willis, D.J. and Peraire, J. (2011). Numerical simulation of flapping wings using a panel method and a high-order Navier-Stokes solver. *International Journal for Numerical Methods in Engineering* **1**: 1–20.
- Polhamus, E. C. (1984). Applying slender wing benefits to military aircraft. *Journal of Aircraft* **21**, 545–559.
- Rayner, J.M.V. (1999). Estimating power curves of flying vertebrates. *Journal of Experimental Biology* **202**, 3449–3461.
- Schmitz F.W. (1942). *Aerodynamics Of The Model Airplane. Part 1. Airfoil Measurements*. Translated at Redstone Scientific Information Center RSIC-721 (1967).
- Simons M. (1999). *Model Aircraft Aerodynamics*. Nexus Special Interests, Hemel Hempstead, UK.
- Swartz, S.M., Iriarte-Diaz, J., Riskin, D.K., Song, A., Tian, X., Willis, D.J. and Breuer, K.S. (2007). Wing structure and the aerodynamic basis of flight in bats. *American Institute of Aeronautics and Astronautics* 10 pp.
- Tholleson, M. and Norberg, U.M. (1991). Moments of inertia of bat wings and body. *Journal of Experimental Biology* **158**, 19–35.
- Tucker, V.A. (1973). Bird metabolism during flight: Evaluation of a theory. *Journal of Experimental Biology* **58**, 689–709.
- Weis-Fogh, T. (1972). Energetics of hovering flight in hummingbirds and in drosophila. *Journal of Experimental Biology* **56**, 79–104.
- Wolken-Mohlmann, G.W., Knebel, P., Baryth, S. and Peinke, J. (2007). Dynamic lift measurements on a FX79W151A airfoil via pressure distribution on the wing tunnel walls. *Journal of Physics: Conference Series* **75**, 012026.